ON THE CAPABILITY OF THE γ-Re_θ TRANSITION MODEL TO PREDICT RELAMINARIZATION

P. Bader [a] - *P. Pieringer* [b] - *W. Sanz* [a]

[a] Institute for Thermal Turbomachinery and Machine Dynamics,
Graz University of Technology
Inffeldgasse 25A, 8010 Graz, Austria. pascal.bader@tugraz.at
[b] Springer und Pieringer EDV Dienstleistungen OG
Haydngasse 7/1 8010 Graz, Austria

ABSTRACT

In flows along solid body surfaces the boundary layer represents the narrow zone between the wall and the free stream where viscous effects are important. Its state of flow (laminar or turbulent) may have strong impact on transport processes like wall friction and heat transfer. These processes influence the efficiency as well as the thermal stress, for example of a turbine blade, and may affect other flow characteristics in a machine as well.
Under certain flow conditions (like strong acceleration), a reverse transition or relaminarization from turbulent to laminar can also occur. In this work, this type of process is numerically analyzed in order to see the capability of the the well-known γ-Re_θ transition model in predicting relaminarization. The model is used together with the Menter SST turbulence model which are both incorporated in the in-house code LINARS.
First, the behavior of the flow during acceleration is analyzed. The results of the present case are compared qualitatively to DNS and measurement results. It is shown, that the transition model successfully predicts relaminarization. Secondly it is found out, which processes inside the boundary layer are triggered by the model allowing us a better understanding how relaminarization is modeled.
The objective of this work reaching a better understanding of the model parameters influencing the relaminarization prediction by the γ-Re_θ transition model will enable an effective future parameter modification in order to enhance the accuracy of the model.

KEYWORDS

Relaminarization, transition modeling, CFD, flat plate testcase

NOMENCLATURE

C	Streamwise extend of the acceleration zone
D/E	Dissipation term
k	Turbulence kinetic energy
k_L	Laminar kinetic energy
K	(Launder) acceleration parameter
P	Production term
$\tilde{Re}_{\theta t}$	Local transition onset momentum-thickness Reynolds number
$Re_{\theta t}$	Transition onset momentum-thickness Reynolds number based on free stream conditions
Tu	Turbulence Intensity

u	Velocity
u^*	Non-dimensional velocity
u^+	Non-dimensional velocity in wall coordinates
u_∞	Local free stream velocity
$u_{\infty,in}$	Free-stream velocity at the inlet
x	Streamwise distance
x_0	Streamwise position of the start of the acceleration zone
y^*	Non-dimensional coordinate
y^+	Non-dimensional wall coordinate
$\delta(x)$	Boundary layer thickness
γ	Intermittency
ν	Kinematic viscosity
ρ	Density
τ_W	Wall shear stress

INTRODUCTION

The boundary layer represents the narrow zone between a solid body wall and the free stream where viscous effects are significant. The state of this boundary layer, whether it is laminar or turbulent, is on one hand influenced by free stream parameters, like the velocity, acceleration or turbulence level of the free stream and on the other hand influences the free stream as well as wall parameters, like skin friction or heat transfer. These parameters may influence for instance the efficiency of a blade and also the thermal stresses which the blade has to withstand. Therefore, an understanding of the state of the boundary layer, i.e. the position, length etc. of the transitional zone, is very important for the designer of turbomachines.

It is vitally important to understand the impact of the influencing parameters on the onset position and length of the transitional zone in order to predict and potentially control the state of the boundary layer. In turbomachinery, the efficiency of blades and stages can be enhanced considering transition. This allows the overall machine performance to be improved. Mayle [1991] published a comprehensive review of the importance of transition in gas turbines. He analyzed experiments performed by several research groups in order to find the influence of different flow parameters on the transition process.

In the last years, additional experiments were performed by many research groups. Yip et al. [1993] performed in-flight measurements, detected transition with the help of Preston tubes and analyzed the influence of the flight conditions on the boundary layer along an air-foil. Oyewola et al. [2003] showed how the flow in the boundary layer can be measured with hot-wire anemometry and Oyewola [2006] Laser-Doppler anemometry (LDA). Widmann et al. [2012] performed near-wall measurements with Particle Image velocimetry (PIV) . Hot-film measurements were performed, e.g., by Mukund et al. [2012], Preston-tube and thermographic measurements by Bader and Sanz [2015a] to investigate the transitional boundary layer. Additionally, Bader et al. [2016b] used Laser Interferometric vibrometry (LIV) to predict transition.

In addition to measurements, numerical models were developed to predict the laminar-turbulent transition process. Established models are, for example, the k-k_L-ω [Walters and Cokljat, 2008] and the γ-Re_θ [Langtry and Menter, 2009] model.

So far, only the transition from laminar to turbulent flow was described. Under certain flow conditions (like strong acceleration), however, a reverse transition or relaminarization from turbulent to laminar can occur. Up to now, only few measurements on relaminarization were

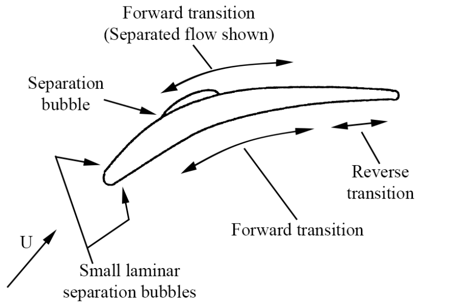

(a) Schematic drawing of a compressor blade.

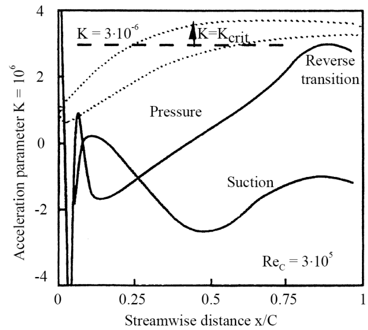

(b) K of a compressor blade.

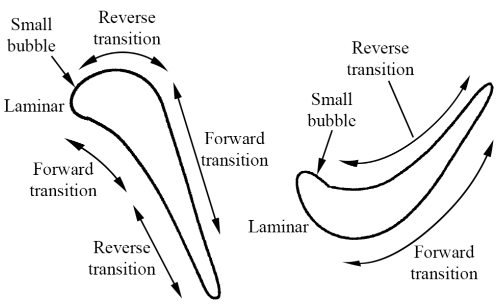

(c) Schematic drawing of a high pressure turbine blade.

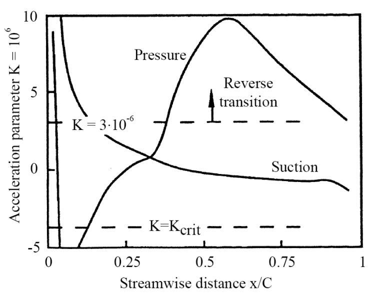

(d) K of a high pressure turbine blade.

Figure 1: Several applications where transition and relaminarization can occur (adopted from Mayle [1991]).

reported (e.g. Narasimha and Sreenivasan [1979], Ichimiya et al. [1998], Escudier et al. [1998], Mukund et al. [2006]). Therefore, at the Institute for Thermal Turbomachinery and Machine Dynamics (ITTM) of Graz University of Technology a project was launched in order to understand the process of relaminarization and its phases even further and test common threshold values for relaminarization by acceleration. First measurements performed at the institute already showed good results and relaminarization was detected [Bader et al., 2016a].

The studies performed within this project and by other research groups are not only applicable to simplified test cases, but they are also important under engine-representative conditions. As Mayle [1991] already showed, transition as well as relaminarization take place on compressor as well as turbine blades. Figures 1a and b, show a schematic drawing of the processes taking place along a compressor blade together with the acceleration parameter K (see Eq. (8)); Figs. 1c and d show the same for a turbine blade. It can be clearly observed, that transition as well as relaminarization occur along a blade, influencing skin friction, heat transfer as well as boundary layer thicknesses which may change the downstream flow angle.

The process of relaminarization has also been extensively analyzed by the works of Fernholz and Warnack [1998] and Warnack and Fernholz [1998] who analyzed axisymmetric turbulent flows under favorable pressure gradients. Their presented DNS studies impressively showed the influence of acceleration on the boundary layer.

Since the processes within the boundary layer are important for the design of turbomachinery, this work deals with the numerical prediction of relaminarization. It has already shown by the authors [Bader and Sanz, 2015b, 2017] that the γ-Re_θ model is able to predict relaminar-

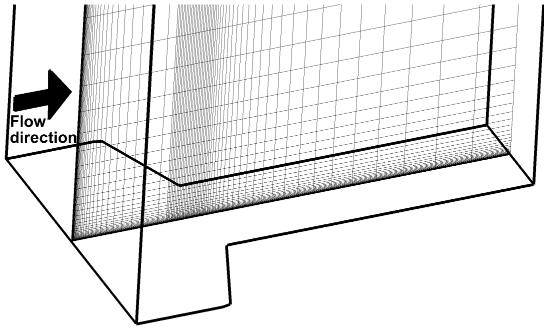

Figure 2: 3D illustration of the quasi-3D mesh.

ization, although there is an uncertainty in the location and streamwise extent. Therefore in this paper it should be investigated, how the model predicts relaminarization in order to be able to modify model parameters in an effective way to improve its prediction capabilities in the future.

The following section presents the numerical setup used for the study. Thereafter we present and discuss the simulation results with a focus on the model parameters. The paper ends with a short summary and the conclusions.

NUMERICAL SETUP

In this work, the CFD simulations have been performed with the in-house code LINARS. LINARS has been developed at Graz University of Technology at the ITTM by Pecnik et al. [2005]. The code solves the Reynolds-averaged Navier-Stokes (RANS) equations in conservative form with a fully-implicit, time-marching finite-volume method. The inviscid (Euler) fluxes are discretized with the upwind flux-difference splitting method of Roe [1981]. The incompressible solutions are obtained with a pseudo-compressibility method.

For the numerical study a generic test case has been designed. The flow along a flat plate was investigated, where the pressure gradient necessary for the acceleration was imposed by a decrease of the cross section in the quasi-3D direction. This has the advantage that no side wall effects like separation or sidewall boundary layer displacement influences the investigated flow along the plate. The structured mesh consists of 6,144 hexaeder elements and is shown in Fig. 2. The streamwise length upstream of the acceleration area has been set in such a way, that the boundary layer is able to fully transit to turbulent flow upstream of the acceleration zone for the calculations where the transition model was used. The y^+ value is kept between 0.1 and 1, which is recommended by Langtry et al. [2004] for the γ-Re_θ transition model.

At the inlet a total pressure of $p = 1.0005$ bar, a total temperature of 300 K and a turbulence intensity of $Tu = 5$ % and $Tu = 12$ %, respectively, depending on the case are imposed. Additionally the integral length scale l was set to 0.0001 m in order to specify the dissipation. At the outlet a static pressure was set, resulting in an inlet speed for all investigated cases of $u_{\infty,in} = 10$ m/s. The chord Reynolds number $Re_C = u_{\infty,in} \cdot C/\nu$, where C represents the length of the plate, is $Re_C = 3 \cdot 10^6$.

As turbulence model the well known SST k-ω turbulence model by Menter [1994] has been used. For modeling transition this turbulence model is coupled with a transition model, namely the γ-Re_θ transition model by Langtry and Menter [2009]. It solves two additional transport equations in order to influence the production and dissipation of the turbulence kinetic energy

k within the turbulence model. The two equations are

$$\frac{\partial(\rho\tilde{Re}_{\theta t})}{\partial t}+\frac{\partial(\rho U_j\tilde{Re}_{\theta t})}{\partial x_j}=P_{\theta t}+\frac{\partial}{\partial x_j}\left[\sigma_{\theta t}(\mu+\mu_t)\frac{\partial\tilde{Re}_{\theta t}}{\partial x_j}\right] \tag{1}$$

$$\frac{\partial(\rho\gamma)}{\partial t}+\frac{\partial(\rho U_j\gamma)}{\partial x_j}=P_\gamma-E_\gamma+\frac{\partial}{\partial x_j}\left[\left(\mu+\frac{\mu_t}{\sigma_f}\right)\frac{\partial\gamma}{\partial x_j}\right] \tag{2}$$

where $\tilde{Re}_{\theta t}$ the local transition onset momentum-thickness Reynolds number and γ represents the intermittency, i.e. the state of transition and varies between zero and one, where one represents fully turbulent flow conditions.

The empirical correlations used for the prediction of transition are based on the idea that after surpassing a critical momentum thickness Reynolds number $Re_{\theta t}$ transition is triggered. But in this way it is a one-dimensional criterion which is only valid along the wall. Therefore Langtry and Menter [2009] introduced the transport variable $\tilde{Re}_{\theta t}$ as a transition criterion which is applicable in the whole flow field. For this reason the production term of the $\tilde{Re}_{\theta t}$ equation is designed in such a way, that $\tilde{Re}_{\theta t}$ is forced to adopt the value of the empirically prescribed transition onset Reynolds number $Re_{\theta t}$ in the free stream. The production term of $\tilde{Re}_{\theta t}$ is defined as

$$P_{\theta t}=c_{\theta t}\rho\frac{\rho U^2}{500\mu}\left(Re_{\theta t}-\tilde{Re}_{\theta t}\right)(1.0-F_{\theta t}) \tag{3}$$

where $Re_{\theta t}$ represents the transition onset momentum-thickness Reynolds number based on free stream conditions. The blending function $F_{\theta t}$ is used to turn off the source term in the boundary layer and allows the transported scalar $\tilde{Re}_{\theta t}$ to diffuse in from the free-stream. $F_{\theta t}$ is equal to zero in the free-stream and one in the boundary layer. [Langtry and Menter, 2009]

The correlation for $Re_{\theta t}$ used by Langtry and Menter [2009] considers the influence of the turbulence intensity Tu and the velocity gradient du/ds on the transition onset.

The production and the dissipation terms of the intermittency γ are defined as

$$P_\gamma = F_{\text{length}}c_{a1}\rho S\left[\gamma F_{\text{onset}}\right]^{0.5}(1-c_{e1}\gamma) \tag{4}$$

$$E_\gamma = c_{a2}\rho\Omega F_{\text{turb}}(c_{e2}\gamma-1) \tag{5}$$

where F_{length} and F_{onset} depend on the local $\tilde{Re}_{\theta t}$ value and determine the length and onset of transition in the flow field. On the other hand F_{turb} only depends on the local turbulence parameters (k and ω). The values of F_{length}, F_{onset} and F_{turb} can vary between $0\leq F_{\text{length}}\leq 40$, $0\leq F_{\text{onset}}\leq 2$ and $0\leq F_{\text{turb}}\leq 1$, respectively.

The coupling of the transition model is done by modifying the original production term P_k and dissipation term D_k of the k equation of the SST turbulence model:

$$\tilde{P}_k=\gamma_{\text{eff}}\,P_k \tag{6}$$

$$\tilde{D}_k=\min(\max(\gamma_{\text{eff}},0.1),1.0)\,D_k \tag{7}$$

RESULTS AND DISCUSSION

As described above a first step is to understand what the transition model does and more important why it can predict relaminarization and what happens during this process. Therefore the results of the generic test-case is presented in this section.

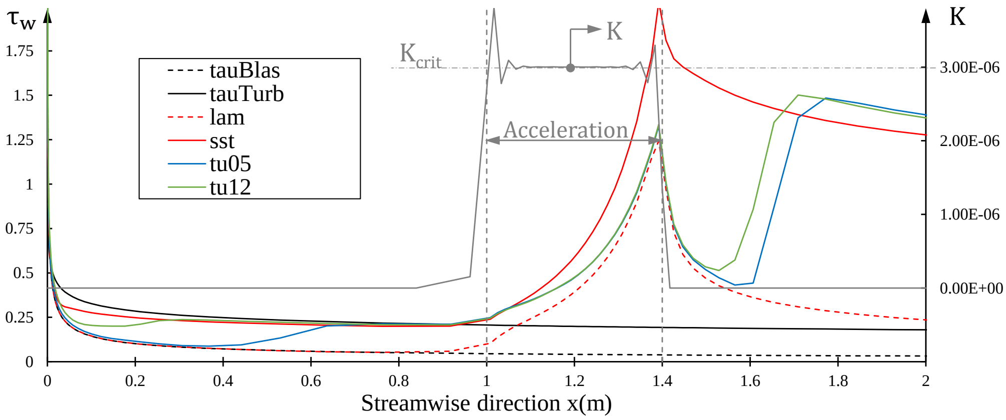

Figure 3: Local wall shear distribution τ_w along the test section.

In a first step it is shown, that relaminarization can be predicted by the transition model. Therefore in Fig. 3 the local wall shear τ_w is given together with the Launder acceleration parameter K. K is defined as

$$K = \frac{\nu}{u_\infty^2} \cdot \frac{du_\infty}{dx} \tag{8}$$

where u_∞ is the local free stream velocity, ν the kinematic viscosity and du_∞/dx the streamwise velocity gradient. According to literature, if this acceleration value surpasses a critical value $K > K_{crit} = 3.0 \cdot 10^{-6}$, relaminarization should most likely occur.

In the figure several curves are given, where the curve labeled as *tauBlas* shows the analytical Blasius (=laminar) solution for zero pressure gradient flow (ZPG), *tauTurb* the empirical turbulent solution for ZPG, *lam* a fully laminar simulation result, *sst* a fully turbulent SST solution, *tu05* and *tu12* a solution with the transition model activated for a free-stream turbulence intensity of $Tu = 5$ % and $Tu = 12$ %, respectively. The turbulence intensity of $Tu = 5$ % was chosen according to the measurement results presented by [Bader and Sanz, 2015b, 2017] and $Tu = 12$ % as an engine relevant value.

The curve for the empirical turbulent solution (ZPG) is defined as

$$\tau_{w,turb} = 0.0577 \cdot \frac{\rho \cdot u_{\infty,in}^2}{2} \cdot Re_x^{-1/5} \tag{9}$$

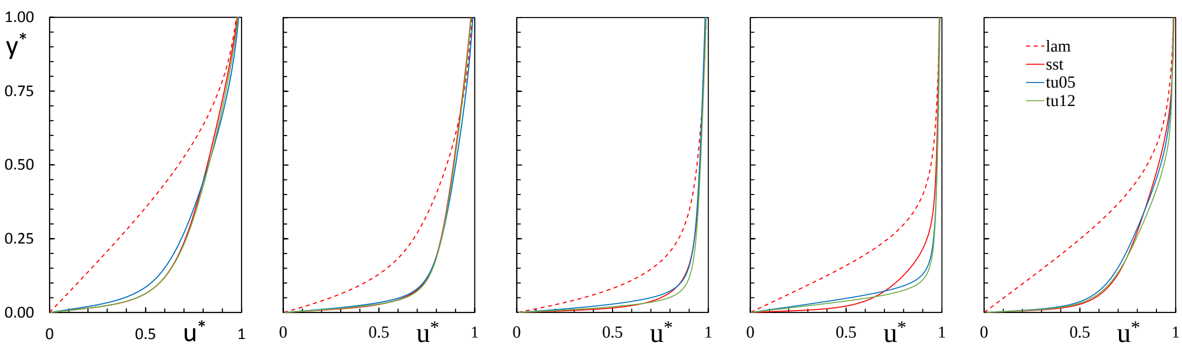

(a) $x = 0.76$ m. (b) $x = 1.11$ m. (c) $x = 1.31$ m. (d) $x = 1.50$ m. (e) $x = 1.93$ m.

Figure 4: Non-dimensional velocity profiles y^* vs. u^* at several x locations.

where $u_{\infty,in}$ represents the velocity at the inlet.

Looking at the results it can be observed that all cases except the fully laminar case (*lam*) are completely turbulent upstream of the acceleration zone. At the beginning of acceleration all curves begin to depart from their analytical/empirical ZPG solutions because the wall shear rises due to the acceleration.

The two curves for the activated transition model (*tu05* and *tu12*) start to differ from the fully turbulent CFD solution where the acceleration parameter K is just above the critical value K_{crit}. During the constant acceleration the two solutions approach the laminar solution, but they never coincide fully. This indicates a laminar-like boundary layer behavior at least close to the wall.

At approximately $x = 1.5$ m the boundary layer of these cases start retransition towards the fully turbulent solution.

It can also be clearly seen, that the free stream turbulence intensity Tu has no influence on the relaminarization, which is surprising, since it has an influence on laminar-to-turbulent transition, which can be seen by their retransitional behavior.

In order to see the change of the velocity distribution within the boundary layer the velocity profiles of the fully laminar (*lam*) and fully turbulent case (*sst*) are given together with the two transitional cases in Figs. 4a to e at different streamwise positions. The profiles are given as non-dimensional velocity profiles $y^* = y/\delta$ against $u^* = u/u_\infty$.

At the first position ($x = 0.76$ m, Fig. 4a) which is upstream of the acceleration, the transitional solution agrees more or less with the fully turbulent solution. At $x = 1.16$ m (Fig. 4b) which is the beginning of acceleration, the fully turbulent solution and the transitional solutions agree well. Fig. 4c shows the profiles at $x = 1.31$ m which represents a position, where according to the τ_w plot the boundary layer is laminar. In the graph it can be seen that close to the wall the transitional solutions coincide more with the laminar solution, whereas at the outer part of the boundary layer the two solutions agree more with the fully turbulent computation. More downstream at $x = 1.50$ m (Fig. 4d), which is already downstream of the acceleration zone, the profiles agree very well with the laminar profile over a larger distance from the wall. Fig. 4e which shows the profile at $x = 1.93$ m where retransition has already occurred, the profiles agree again with the fully turbulent solution in the near-wall region.

Additionally the results of the present simulation are compared qualitatively to the DNS data of Warnack and Fernholz [1998]. Therefore the velocity profiles are given in wall coordinates y^+/u^+ defined as

$$y^+ = \frac{y \cdot u_\tau}{\nu} \tag{10}$$

$$u^+ = \frac{u}{u_\tau} \tag{11}$$

where $u_\tau = (\tau_w/\rho)^{1/2}$ represents the friction velocity. The profiles in wall coordinates are given in Fig. 5a to e at the same streamwise positions as in Fig. 4 for the present simulation and in Fig. 5f the results of Warnack and Fernholz [1998] are given[1]. Additionally the $y^+ = u^+$ and $u^+ = 1/\kappa \ ln(y^+) + B^+$ profiles are given as laminar and turbulent reference, respectively.

At the first position ($x = 0.76$ m) one can clearly observe, that the transitional solutions agree with the fully turbulent one. Within the acceleration zone a typical behavior of all profiles

[1] Colored lines have been added to the DNS data for optical guidance, but only for profiles upstream of the retransition position

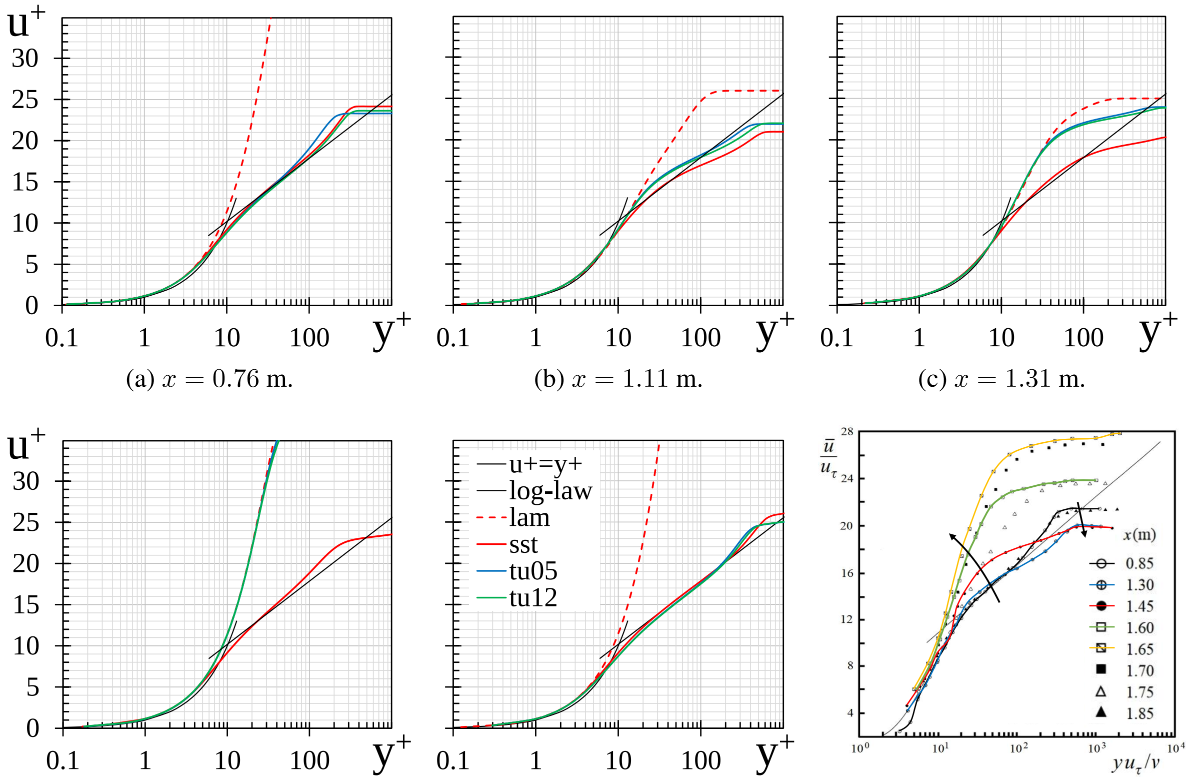

(a) $x = 0.76$ m. (b) $x = 1.11$ m. (c) $x = 1.31$ m.

(d) $x = 1.50$ m. (e) $x = 1.93$ m. (f) DNS of Warnack and Fernholz [1998] (color lines added for optical guidance).

Figure 5: Velocity profiles in wall coordinates y^+ vs. u^+ at several x locations together with the DNS results of Warnack and Fernholz [1998].

can be observed: Due to the strong FPG the outer part of the profiles ($y^+ > 100$) drops below the log-law. This behavior has also been observed by Warnack and Fernholz [1998] and is indicated by the right arrow in Fig. 5f which shows the change of the black to the blue profile. At $x = 1.11$ m it can be additionally observed that the transitional cases agree with the fully laminar one at the inner part of the boundary layer (up to $y^+ \approx 12$). We can therefore conclude, that relaminarization begins at the inner part of the boundary layer. The extend of this inner zone of good agreement between the laminar and transitional cases grows with streamwise position until these three curves agree with each other. This again agrees with the observations of Warnack and Fernholz [1998] (second arrow in Fig. 5f showing the change of the blue profile over the red and green one to the yellow one). At $x = 1.93$ m both transitional cases are fully turbulent again, thus agreeing with the SST solution.

To sum up, the wall shear stress and the velocity profiles have shown that the model is able to predict relaminarization. The behavior during relaminarization and retransition computed by the γ-Re_θ transition model agrees qualitatively well with published measurements [Bader et al., 2016a] and DNS data [Warnack and Fernholz, 1998].

In the following it should be explained how the relaminarization process is triggered within the transition model. Therefore in Fig. 6 the contour plots of several properties together with iso-lines are shown for the transitional case with a turbulence intensity of $Tu = 12$ %.

In Fig. 6a the intermittency γ is presented together with the boundary layer thickness $\delta(x)$

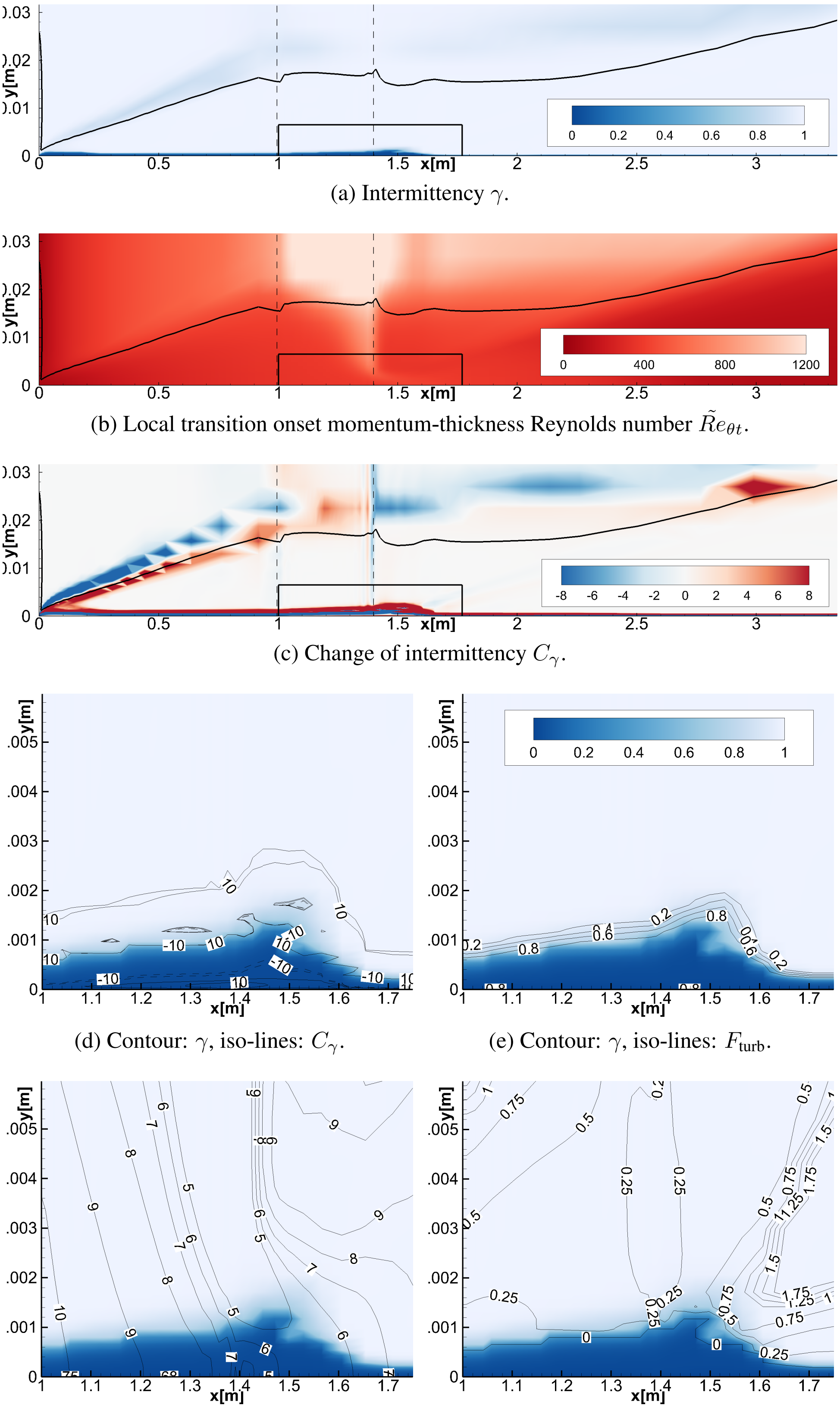

(a) Intermittency γ.

(b) Local transition onset momentum-thickness Reynolds number $\tilde{Re}_{\theta t}$.

(c) Change of intermittency C_γ.

(d) Contour: γ, iso-lines: C_γ.

(e) Contour: γ, iso-lines: F_{turb}.

(f) Contour: γ, iso-lines: F_{length}.

(g) Contour: γ, iso-lines: F_{onset}.

Figure 6: Contour plots at midspan.

(solid black line), which is defined as $u(y = \delta) = 0.99u_\infty$. It can be seen, that the intermittency in most parts of the boundary layer is approximately 1, only a small part close to the wall shows $\gamma = 0$. This small area represents the laminar sublayer. Within the acceleration zone (within the dashed black lines) this laminar sublayer increases its height in the latter part of this zone. This on the other hand leads to a reduction of the velocity gradient close to the wall which reduces the wall shear. This agrees with the observations above. The question is, what triggers this thickening of the inner part of the boundary layer and why it has a streamwise delay compared to the acceleration.

To answer these questions, $\tilde{Re}_{\theta t}$ is given in Fig. 6b. It can be clearly seen, that the value and thus the transition threshold rises in response to the acceleration in the free-stream, but as discussed above $\tilde{Re}_{\theta t}$ needs some streamwise distance in order to diffuse to the inner boundary layer. This delay fits to the delay of the thickening of the low-γ-zone described above. Downstream of the acceleration, $\tilde{Re}_{\theta t}$ decrease again, promoting retransition.

As shown above, $\tilde{Re}_{\theta t}$ influences the production term of the intermittency P_γ. On the other hand, the turbulent variables (F_{turb}) influence the dissipation term E_γ. In order to see which is dominating, Fig. 6c shows the source term of the γ equation C_γ defined as

$$C_\gamma = P_\gamma - E_\gamma. \tag{12}$$

Focusing on the behavior of C_γ close to the wall in Fig. 6c it can be seen that there is a high dissipation close to the wall were the thickening of the inner layer takes place. Just outside of this zone there is a high production of γ. To see this in more detail, Fig. 6d gives the intermittency as contour plot together with the source term C_γ as a magnified view of the black box in Figs. 6a to c. It can be clearly seen, that the area of destruction (negative C_γ) fits to the low-γ area, whereas the area of higher C_γ fits to areas with $\gamma \approx 1$.

As shown in Eq. (5) the dissipation depends on the factor F_{turb}. In Fig. 6e the iso-lines of this value are illustrated together with the intermittency γ as contour plot. It can be seen, that F_{turb} reaches its maximum value close to the wall, leading to a high dissipation. The shape of this high F_{turb} zone agrees well with the shape of the low-γ zone close to the wall.

The production of γ depends on the factors F_{length} and F_{onset} (compare Eq. (4)). These two values are influenced by - beside others - the local transition onset momentum-thickness Reynolds number $\tilde{Re}_{\theta t}$. The iso-lines of these two factors are given in Figs. 6f and g, respectively, with the contour plot of γ. It can be clearly seen that both values decrease with the increase of $\tilde{Re}_{\theta t}$ shown in Fig. 6b. This leads to a reduction of the production in this area. Together with the higher dissipation described above this results in a thickening of the inner laminar layer. At approximately $x \approx 1.65$ m where $\tilde{Re}_{\theta t}$ decreases again, F_{length} and F_{onset} increase. This leads to a high production of γ promoting the fast retransition explained earlier in this work.

To sum up, the acceleration leads to a rise of $\tilde{Re}_{\theta t}$ outside the boundary layer. This rise is then transported into the boundary layer and leads in the rear part of the acceleration to a drop of F_{length} and F_{onset}. This drop reduces the production of γ. On the other hand F_{turb}, which is not influenced by $\tilde{Re}_{\theta t}$ but by the turbulence values, rises which leads to a higher dissipation of γ. These two effects yield a thickening of a low-γ-region close to the wall and ultimately to a decrease of the velocity gradient, thus wall shear.

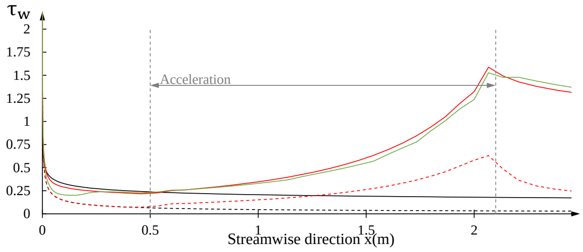

(a) $K = 7.5 \cdot 10^{-7}$.

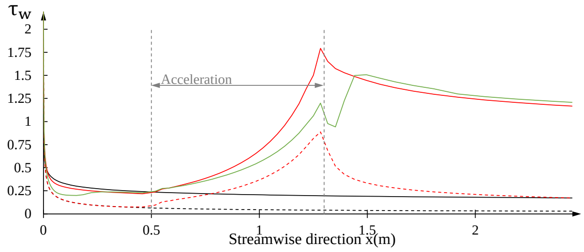

(b) $K = 1.5 \cdot 10^{-6}$.

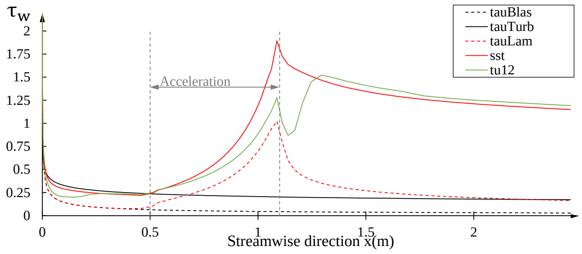

(c) $K = 2.25 \cdot 10^{-6}$.

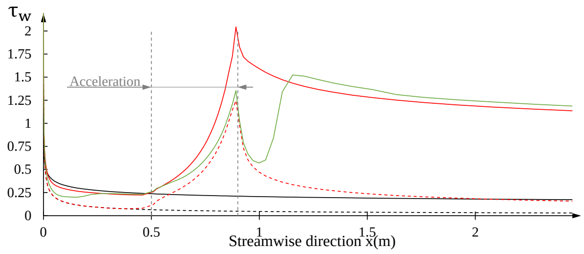

(d) $K = 3.0 \cdot 10^{-6}$.

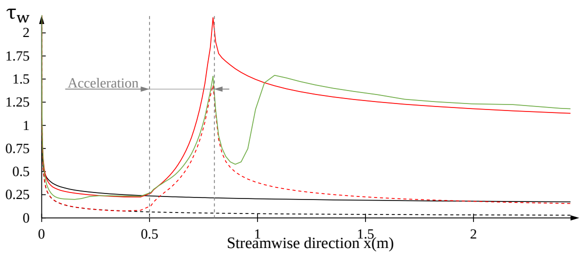

(e) $K = 4.0 \cdot 10^{-6}$.

Figure 7: Local wall shear distribution τ_w along the test section for different acceleration parameters K.

Influence of K on relaminarization prediction

As discussed above, the acceleration parameter K is considered as a critical parameter for relaminarization by acceleration. According to literature relaminarization occurs when the value surpasses $3 \cdot 10^{-6} \leq K_{crit} \leq 3.5 \cdot 10^{-6}$ [Bardi Narayanan and Ramjee, 1969, Blackwelder and Kovasznay, 1972, Narasimha and Sreenivasan, 1979, Mayle, 1991, Ichimiya et al., 1998, Escudier et al., 1998, Mukund et al., 2006]. Therefore a study was performed to see how the model reacts on the acceleration parameter. The variation of K has been done with a change of the acceleration length at the same inlet and outlet conditions and an inlet turbulence of $Tu = 12\%$.

Figure 7a to e shows different distributions of the wall shear τ_w along the streamwise coordinate x. The given curves in the figures represent the fully turbulent, transitional and fully laminar solution for acceleration parameters from $K = 7.5 \cdot 10^{-7}$ up to $K = 4.0 \cdot 10^{-6}$, and additionally the laminar and fully turbulent solution for zero-pressure-gradient flow.

At first, it is interesting to notice that the wall shear at the end of acceleration for the fully laminar and fully turbulent solution increases significantly with increasing acceleration parameter and thus decreasing length of acceleration. The reason for this behavior is that the boundary layer needs some flow length to adapt to the increasing free-stream velocity which is less available the shorter the acceleration zone is. This is visible by the decrease of wall shear after the acceleration zone where the boundary layer has time to adapt to the higher free-stream velocity. But within the acceleration zone the gradient between boundary layer flow and free-stream flow increases the shorter the acceleration length is.

Regarding relaminarization prediction the trend of the transitional solution in relation to the fully turbulent and fully laminar solution is of interest. It can be seen, that the case with the lowest K-value ($K = 7.5 \cdot 10^{-7}$, Fig 7a) shows nearly no relaminarization and behaves similar to the fully turbulent solution. With increasing K (Figs. 7b and c) , the solutions tend more and more towards their laminar CFD solutions. When K reaches its stated critical value of $3.0 \cdot 10^{-6}$ (Fig. 7d), the local wall shear stress τ_w nearly fully approaches the laminar solution. If the acceleration is increased further above the critical value, nearly no difference regarding relaminarization can be observed. Thus the transition model is well calibrated to the critical value of $K = 3.0 \cdot 10^{-6}$. But the model also shows relaminarization in a weaker form for K values below the critical value.

Downstream of the acceleration zone, all cases which showed partial or full relaminarization show retransition at the same position, at approximately $\Delta x \approx 0.1$ m downstream of the end of the acceleration zone.

SUMMARY AND CONCLUSIONS

In this work a numerical study has been presented which gives a deep insight into the mechanism leading to relaminarization in the γ-Re_θ transition model making it capable of predicting relaminarization. The predicted behavior of the boundary layer velocity profiles has been also found from DNS calculations published. It has been found, that the local transition onset momentum-thickness Reynolds number $\tilde{Re}_{\theta t}$ rises due to acceleration. This rise causes the model parameters F_{length} and F_{onset} to drop, leading to a reduction of the production of the intermittency γ together with an increase of the intermittency dissipation E_γ. The resulting lower intermittency γ then leads to a decrease of the turbulence kinetic energy and thus to a reduced velocity gradient close to the wall and wall shear. This is visible by a change of the shape of the velocity profile in the boundary layer.

The following analysis of the influence of different acceleration parameters K on the relaminarization prediction showed, that the critical value of K stated in the literature is also well considered in the transition model. A higher K value only marginally changes the relaminarization behavior whereas for smaller K values partial relaminarization is also predicted by the simulation. Only for very low K values the flow remains fully turbulent.

So it can be concluded that the γ-Re_θ transition model can be also applied to highly accelerated flows where relaminarization can occur, but further calibration of the model with measurement data is recommended.

ACKNOWLEDGEMENTS

The authors gratefully acknowledge financial support from the Austrian Federal Ministry for Transport, Innovation and Technology in funding the work by the project RELAM within the Austrian Aeronautics Program TAKE OFF.

REFERENCES

P. Bader and W. Sanz. On the setup of a test bench for predicting laminar-to-turbulent transition on a flat plate. *Proceedings of the 12th International Symposium on Experimental Computational Aerothermodynamics of Internal Flows, Genova, Italy*, 2015a. ISAIF12-074.

P. Bader and W. Sanz. Measurement and simulation of flat-plate boundary layers in accelerated flow. *Poster presentation at ASME 2015 Turbo EXPO, Montreal, Canada*, 2015b. GT2016-58198.

P. Bader and W. Sanz. Measurements and simulation of a turbulent boundary layer exposed to acceleration along a flat plate. *Proceedings of 12th European Conference of Turbomachinery Fluid Dynamics & Thermodynamics ETC12*, April 2017. ETC2017-92.

P. Bader, M. Pschernig, W. Sanz, J. Woisetschläger, F. Heitmeir, W. Meile, and G. Brenn. Flat-plate boundary layers in accelerated flow. *Proceedings of ASME Turbo Expo 2016: Turbine Technical Conference and Exposition, Seoul, South Korea*, 2016a. GT2016-56044.

P. Bader, W. Sanz, J. Peterleithner, J. Woisetschläger, F. Heitmeir, W. Meile, and G. Brenn. Detecting transition on flat plate flow with laser interferometric vibrometry (LIV). *Proceedings of ASME Turbo Expo 2016: Turbine Technical Conference and Exposition, Seoul, South Korea*, 2016b. GT2016-56043.

M. A. Bardi Narayanan and V. Ramjee. On the criteria for reverse transition in a two–dimensional boundary layer. *Journal of Fluid Mechanics*, 35:225–241, 1969.

R. F. Blackwelder and L. S. G. Kovasznay. Large–scale motion of a turbulent boundary layer during relaminarization. *Journal of Fluid Mechanics*, 53:61–83, 1972.

M. P. Escudier, A. Abdel-Hameed, M. W. Johnson, and C. J. Sutcliffe. Laminarisation an re–transition of a turbulent boundary layer subjected to favourable presser gradient. *Experiments in Fluids*, 25:491–502, 1998.

H. H. Fernholz and D. Warnack. The effects of a favourable pressure gradient and of the reynolds number on an incompressible axisymmetric turbulent boundary layer. part 1: The turbulent boundary layer. *Journal of Fluid Mechanics*, 359:329–356, 1998.

M. Ichimiya, I. Nakamura, and S. Yamashita. Properties of a relaminarizing turbulent boundary layer under a favorable pressure gradient. *Experimental Thermal and Fluid Science*, 17: 37–48, 1998.

R. B. Langtry and F. R. Menter. Correlation-based transition modeling for unstructured parallelized computational fluid dynamics codes. *AIAA Journal*, 47(12):2894–2906, 2009.

R. B. Langtry, F. R. Menter, S. R. Likki, Y. B. Suzen, P. G. Huang, and S. Völker. A correlation based transition model using local variables part 2: Test cases and industrial applications. *Proceedings of ASME 2004 Turbo EXPO, Vienna, Austria*, 2004. GT2004-53454.

R. E. Mayle. The role of laminar-turbulent transition in gas turbine engines. *Journal of Turbomachinery*, 113(4):509–537, October 1991.

F. R. Menter. Two-equation eddy-viscosity turbulence models for engineering applications. *AIAA Journal*, 32(8):1598–1605, 1994.

R. Mukund, P. R. Viswanath, R. Narasimha, A. Prabhu, and J. D. Crouch. Relaminarization in highly favourable pressure gradients on a convex surface. *Journal of Fluid Mechanics*, 566: 97–115, 2006.

R. Mukund, R. Narasimha, P. R. Viswanath, and J. D. Crouch. Multiple laminar-turbulent transition cycles around a swept leading edge. *Experiments in Fluids*, 53:1915–1927, 2012.

R. Narasimha and K. R. Sreenivasan. Relaminarization of fluid flows. *Advances in applied mechanics*, 61:221–309, 1979.

O. Oyewola. LDV measurements in a pertubed turbulent boundary layer. *Journal of Applied Science*, 6(14):2952–2955, 2006.

O. Oyewola, L. Djenidi, and R. A. Antonia. Combined influence of the reynolds number and localised wall suction on a turbulent boundary layer. *Experiments in Fluids*, 35:199–206, July 2003.

R. Pecnik, P. Pieringer, and W. Sanz. Numerical investigation of the secondary flow of a transonic turbine stage using various turbulence closures. *In Proceedings of ASME Turbo Expo 2005, Reno-Tahoe, Nevada, USA*, 2005. GT2005-68754.

P. L. Roe. Approximate riemann solver, parameter vectors and differencing scheme. *Journal of Computational Physics*, 43:357–372, 1981.

K. Walters and D. Cokljat. A three-equation eddy-viscosity model for reynolds-averaged navier-stokes simulations of transitional flows. *Journal of Fluids engineering*, 130:1214011–12140114, 2008.

D. Warnack and H. H. Fernholz. The effects of a favourable pressure gradient and of the reynolds number on an incompressible axisymmetric turbulent boundary layer. part 2: The boundary layer with relaminarization. *Journal of Fluid Mechanics*, 359:357–381, 1998.

A. Widmann, A. Duchmann, A. Kurz, S. Grundmann, and C. Tropea. Measuring tollmien-schlichting waves using phase-averaged particle image velocimetry. *Experiments in Fluids*, 53:707–715, 2012.

L. P. Yip, P. Vijgen, J. D. Hardin, and C. P. van Dam. In-flight pressure distributions and skin-friction measurements on a subsonic transport high-lift wing section. *AGARD CP-515*, 1993.